Rectification and stability of a single molecular diode with controlled orientation

Ismael Díez-Pérez[1], Joshua Hihath[1], Youngu Lee[2†], Luping Yu[2]*, Lyudmyla Adamska[3], Mortko A. Kozhushner[4], Ivan I. Oleynik[3] and Nongjian Tao[1]*

In the molecular electronics field it is highly desirable to engineer the structure of molecules to achieve specific functions. In particular, diode (or rectification) behaviour in single molecules is an attractive device function. Here we study charge transport through symmetric tetraphenyl and non-symmetric diblock dipyrimidinyldiphenyl molecules covalently bound to two electrodes. The orientation of the diblock is controlled through a selective deprotection strategy, and a method in which the electrode–electrode distance is modulated unambiguously determines the current–voltage characteristics of the single-molecule device. The diblock molecule exhibits pronounced rectification behaviour compared with its homologous symmetric block, with current flowing from the dipyrimidinyl to the diphenyl moieties. This behaviour is interpreted in terms of localization of the wave function of the hole ground state at one end of the diblock under the applied field. At large forward current, the molecular diode becomes unstable and quantum point contacts between the electrodes form.

Chemistry plays a key role in the emerging field of molecular electronics because the capability of engineering the structure of molecules to achieve the desired properties is paramount to success in this field. These properties include intrinsic electronic device functions as well as a molecules' ability to interact with electrodes and to assemble into molecular junctions. One of the most exciting device functions, the diode (or rectification) behaviour was first envisioned by Aviram and Ratner[1]. The Aviram–Ratner molecular diode consists of a donor and an acceptor separated with a σ bridge in which the forward current is from the acceptor to the donor. To date most experimental studies of molecular diodes have been carried out using Langmuir–Blodgett films[2] and self-assembled monolayers (SAMs)[3], which involve many molecules. In comparison, the diode behaviour in single molecules has been studied much less[4].

To achieve a single-molecule rectification effect, we must (1) provide a reliable and symmetric contact between a non-symmetric molecule and two electrodes, and (2) be able to determine and control the orientation of the molecule relative to the polarity of the applied bias voltage. Reliable and symmetric contacts can be achieved with covalent binding between two terminal groups of the molecule and two metal electrodes, allowing for the statistical analysis of the charge transport of thousands of repeatedly formed metal–molecule–metal junctions using a mechanically controlled break-junction technique[5] or a scanning tunnelling microscope (STM) break-junction technique[6]. However, the orientation of the molecule with respect to the polarity of the bias is difficult to control and determine using these methods.

In this work, an alternating current (a.c.) distance-modulated signal is implemented into the STM break-junction technique and combined with selective deprotection of the molecule's terminal groups to measure unambiguously the current–voltage (I–V) characteristics of single molecules and to control their orientation. Using this approach, we measured the conductance of structurally similar molecular blocks (Fig. 1a,b), observed a pronounced

rectification in the non-symmetric one and studied the stability of this single-molecule diode at large forward currents. The observed rectification is interpreted in terms of non-symmetric localization of the wave function of the hole ground state of the diblock in the applied electric field. The results demonstrate that symmetry breakdown in a molecule introduced by chemical substitution gives rise to a dramatic change in the charge transport and leads to large rectification. Moreover, appropriate engineering of the protection groups of the molecule allows control of the molecular orientation.

The diode candidate studied is a dipyrimidinyl–diphenyl diblock (Fig. 1b). The molecule consists of an electron-deficient bipyrimidinyl moiety covalently connected to an electron-rich biphenyl block, which resembles a p–n junction of a semiconductor device, and so makes it attractive for molecular diode studies[7,8]. A tetraphenyl block, a fully symmetric molecule that is structurally similar to the non-symmetric diblock (Fig. 1a), was also studied to demonstrate that the substitution of a biphenyl by a bipyrimidinyl moiety can lead to large and controlled changes in the charge-transport properties of the molecules. The a.c.-assisted STM break-junction method involves modulation of the distance between the STM tip and the substrate at a high frequency with a simultaneous measurement of the a.c. and direct current (d.c.) components of the current response. The amplitude of the a.c. response allows us to determine whether a molecule is bridged between the tip and substrate electrodes, whereas the d.c. component measures the I–V characteristics of the single-molecule junctions.

To determine the molecular orientation relative to the bias, two strategies were used. Initially, the non-symmetric molecule was terminated with two different protecting groups, trimethylsilylethyl and cyanoethyl (see Methods), attached to the dipyrimidinyl and diphenyl ends of the molecule, respectively. The first deprotection step removed the cyanoethyl protecting group, which allowed a SAM to form on the gold substrate of the diblock non-symmetric molecules with the diphenyl end bound to the substrate electrode. The second step removed the trimethylsilylethyl group, which
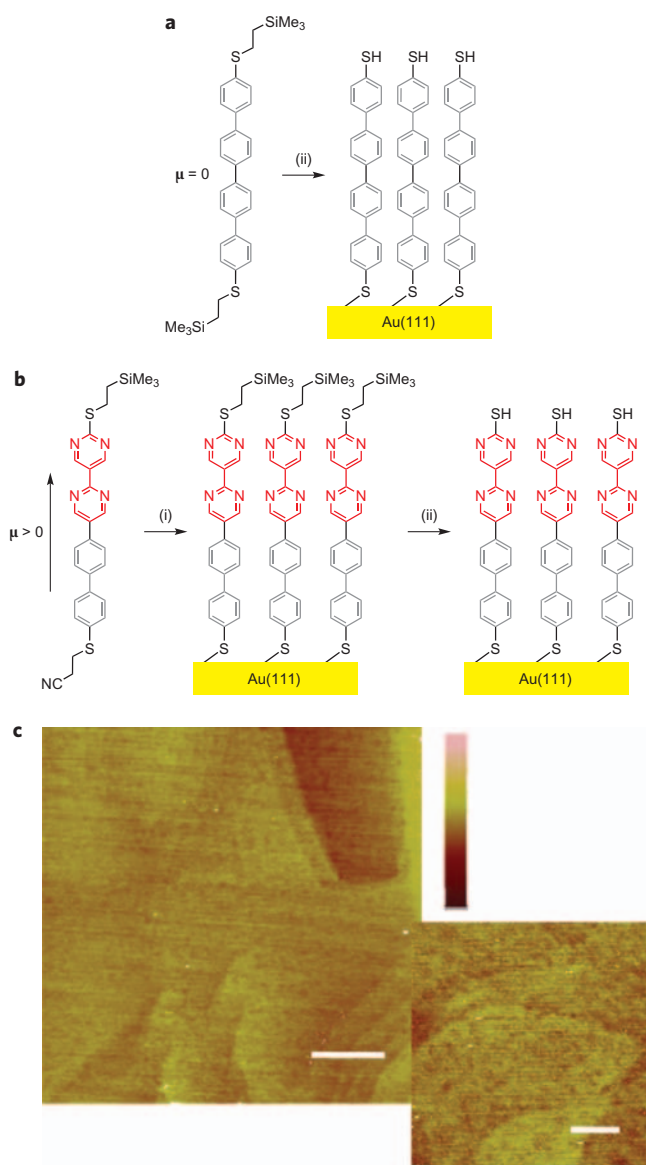
Figure 1 | Preparation of the SAMs. a,b, Symmetric tetraphenyl molecule (**a**) and non-symmetric dipyrimidinyl–diphenyl molecule (**b**). The reagents used were (i) sodium ethoxide, ethanol and THF, and (ii) tetrabutylammonium fluoride and THF. The vertical arrow next to the molecule in (**b**) indicates presence of a dipole moment (**μ**) along the molecular axis. **c,** Constant-current STM images of the SAM; scale bars 50 and 25 nm (inset). Setpoint current 0.3 nA, bias voltage −50 mV and Z bar 2 nm.

exposes the thiol group at the dipyrimidinyl end to the tip electrode (Fig. 1b). Pin holes observed on the STM images in Fig. 1c show evidence that a SAM has formed. The effectiveness of this deprotection method has been characterized previously using infrared spectroscopy[8]. To preserve the molecular orientation during the measurement, the a.c.-assisted method was subsequently applied by gradually moving the tip towards the substrate, starting from a large distance.

First-principle calculations of the I–V characteristics were also performed based on density functional theory, and compared with the experimental results.

Results and discussions

To determine the conductance (G) of the molecules, STM break-junction measurements were performed at low bias voltages (<150 mV). Figure 2a (graphs i,ii) shows plots of several individual current traces recorded during the retraction of the STM tip from

the substrate at different voltage biases (see Methods) in the presence of the symmetric tetraphenyl block, and shows plateaus that correspond to the formation of single-molecule junctions[6,9,10]. Control experiments carried out in a solution that contained no target molecules exhibited smooth exponential decays because of tunnelling through the solvent (Fig. 2a, graph iii). Statistical analysis of the positions of the plateaus in thousands of current traces resulted in histograms with peaks that were used to determine the single-molecule conductance of the symmetric tetraphenyl block (Fig. 2c). From the peak position, the conductance of the molecule was found to be $4.5 \times 10^{-5}\ G_0$, where $G_0 = 2e^2/h = 77.4\ \mu S$ (e is the electron charge and h the Planck constant). The conductance value is consistent with that obtained for shorter symmetric oligophenyl ($n \leq 3$) systems[9,11,12]. Similar measurements were carried out for the non-symmetric dipyrimidinyl–diphenyl moiety (Fig. 2b,d). The measured conductance for the non-symmetric molecule was $1.5 \times 10^{-4}\ G_0$. This value is three times larger than that for the symmetric molecule, even though both systems are similar in length and structure.

Individual current traces obtained at different bias voltages show plateaus associated with the formation of single-molecule junctions (Fig. 2a,b, graphs i,ii). The current values of the plateaus increase linearly with the bias, as expected for the low bias range of voltages. In principle, I–V characteristics of a molecular junction could be obtained by measuring the peak positions in the conductance histograms as a function of bias. However, the statistical average over many molecules with different orientations washes out rectification and other detailed features. Another difficulty with this statistical approach is that the plateaus in the individual current traces become increasingly noisy as bias is increased because of current-induced instability, which makes it difficult to obtain clear peaks in the conductance histograms. Direct measurement of I–V characteristics by sweeping the bias for each individual molecular junction provides more information and could be carried out using mechanically controlled break-junction or STM break-junction methods. However, molecular orientation in these break-junction experiments is not controlled. The static a.c.-modulation method, when combined with the sequential two-step chemical deprotection, allows us not only to measure unambiguously the I–V characteristics of a single-molecule junction, but also to determine the orientations of the non-symmetric molecules relative to the polarity of the applied bias.

The static a.c.-modulation method can be implemented easily with the STM break-junction technique. If no molecules are bridged between the tip and substrate electrodes, then the measured current is dominated by electron tunnelling through the solvent, which decays exponentially with the tip–substrate distance with a large decay constant. So a small modulation in the tip–substrate distance leads to a large amplitude in the current response. In contrast, if a molecule bridges the tip and substrate electrodes, then the current is dominated by conduction through the molecule. When the tip–substrate distance is modulated, the deformation mostly takes place at the soft gold–gold bonds at the molecule–electrode contact, which doesn't greatly affect the conductance of the molecule. Stretching/compressing of the molecule itself also occurs, but to a much lesser extent. Taken together, these two contributions have a much weaker dependence on a small modulation in the tip–substrate distance than electron tunnelling through the solvent does[13]. The modulated amplitude of the tip–substrate distance is kept much smaller than the bond length, so that the a.c. modulation does not greatly affect the stability of the molecular junction[14] (see Methods). Furthermore, with high-frequency a.c. modulation it is straightforward to measure both the d.c. and the a.c. components simultaneously[15]. The d.c. component provides the usual conductance and I–V measurements, whereas the a.c. component serves as an indicator to determine whether a molecule is bound between the tip and substrate.
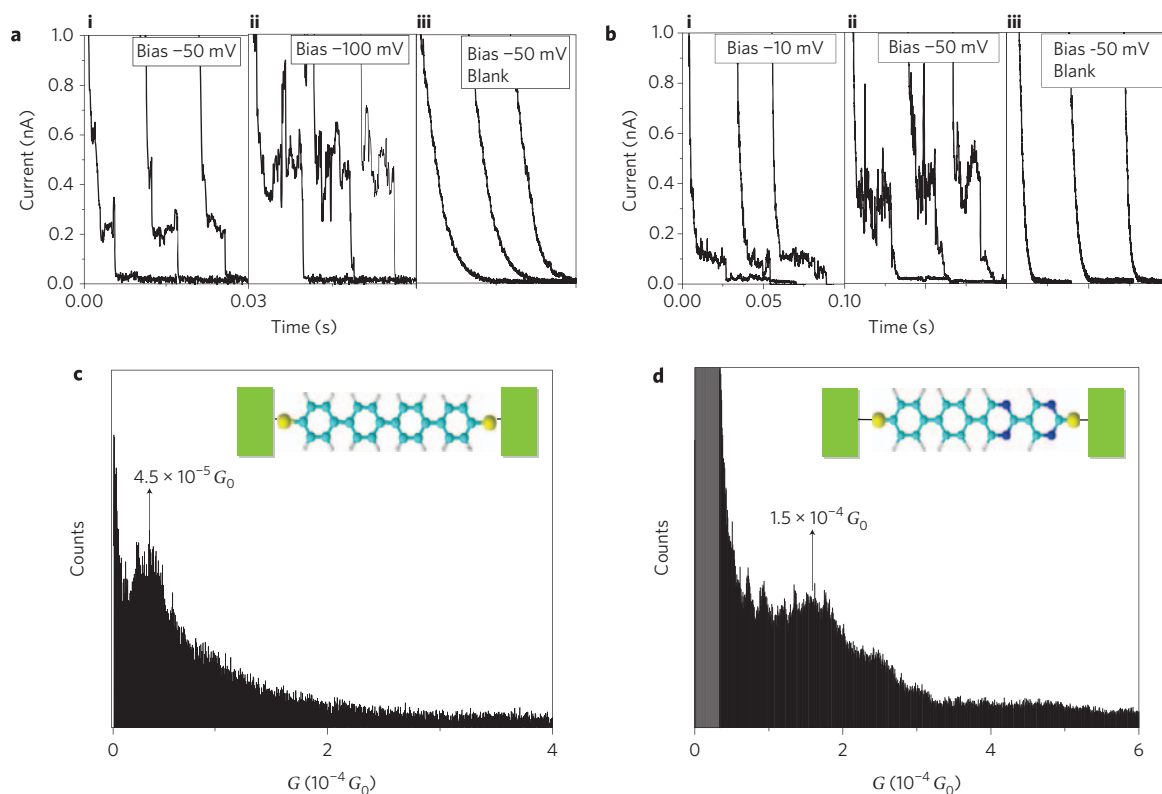
Figure 2 | Current traces and conductance histograms for the symmetric and non-symmetric molecules. a,b, Individual current traces during break-junction measurements at different bias voltages for the tetraphenyl (**a**) and dipyrimidinyl–diphenyl (**b**) molecules (C, light blue; N, dark blue). The current traces in the absence of molecule are shown in graph **iii** in (**a**) and (**b**). **c,d,** Conductance histograms for tetraphenyl (**c**) and dipyrimidinyl–diphenyl (**d**) molecules, respectively ($V_{bias} = -50$ mV). S, yellow; H, white; C, light blue; N, dark blue; gold electrodes, green bars.

To illustrate the a.c.-modulation method, we monitored the a.c. response at different tip–substrate distances in the presence of octanedithiol molecules (Supplementary Fig. S2). When the tip–substrate distance is large compared with the molecular length (see Supplementary Fig. S2a,b), the a.c. amplitude is large with a normalized value close to 10 nm^{-1}. Here the normalized a.c. amplitude is defined by $(\Delta I/I)/L$, where ΔI is the amplitude of the a.c. response, I is the d.c. component and L is the amplitude of the applied modulation; $(\Delta I/I)/L$ corresponds to the tunnelling decay constant, β, for a tunnelling gap. When the tip–sample distance decreases, abrupt switching of the a.c. amplitude to a lower level, for example 2–4 nm^{-1}, is observed, which indicates the formation of a molecular bridge or junction (see Supplementary Fig S2c,d). Figure 3 shows simultaneously recorded a.c. (upper trace) and d.c. components (lower trace) for the non-symmetric dipyrimidinyl–diphenyl molecule. Switching of the a.c. response to a lower level occurs when a molecule bridges between the substrate and the tip (regime B in Fig. 3). At the same time, the d.c. jumps into a higher level, as previously reported[16]. The a.c. amplitude is then used to determine whether a molecule is bridged between two electrodes and the concurrent increase in the d.c. measures the conductance of the molecular junction. The d.c. jump, as shown in Fig. 3, is 0.54 ± 0.11 nA at a bias of -50 mV, which corresponds to a conductance of $(1.39 \pm 0.28) \times 10^{-4}$ G_0, which is consistent with the single-molecule conductance determined from the peaks in the histograms[17].

The a.c. amplitude switches stochastically between two values and can last for many seconds in each state at room temperature, which allows us to record I–V curves in either of the two states. Figure 4a shows I–V curves recorded in the presence of the symmetric molecule when the a.c. amplitude is in the high (black
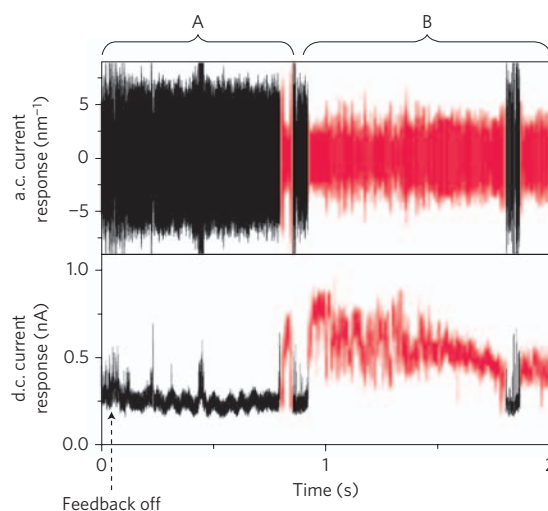

Figure 3 | Components of the current traces during a single dipyrimidinyl-diphenyl bridge formation. Regions A (black) and B (red) correspond to tunnelling by means of space and conduction, respectively, through the single-molecule junction. The dashed arrow indicates when the feedback was turned off. The initial setpoint current was 0.25 nA and the bias was 50 mV. The amplitude and frequency of the a.c. modulation were 0.06 nm and 2 kHz, respectively. The a.c.-response (nm^{-1}) is a normalized value as defined in the text.

curve) or low (red curve) level. In the high level one end of the molecule is connected to an electrode (Fig. 4a, insets), but in the low level the molecule is connected covalently to both the tip and
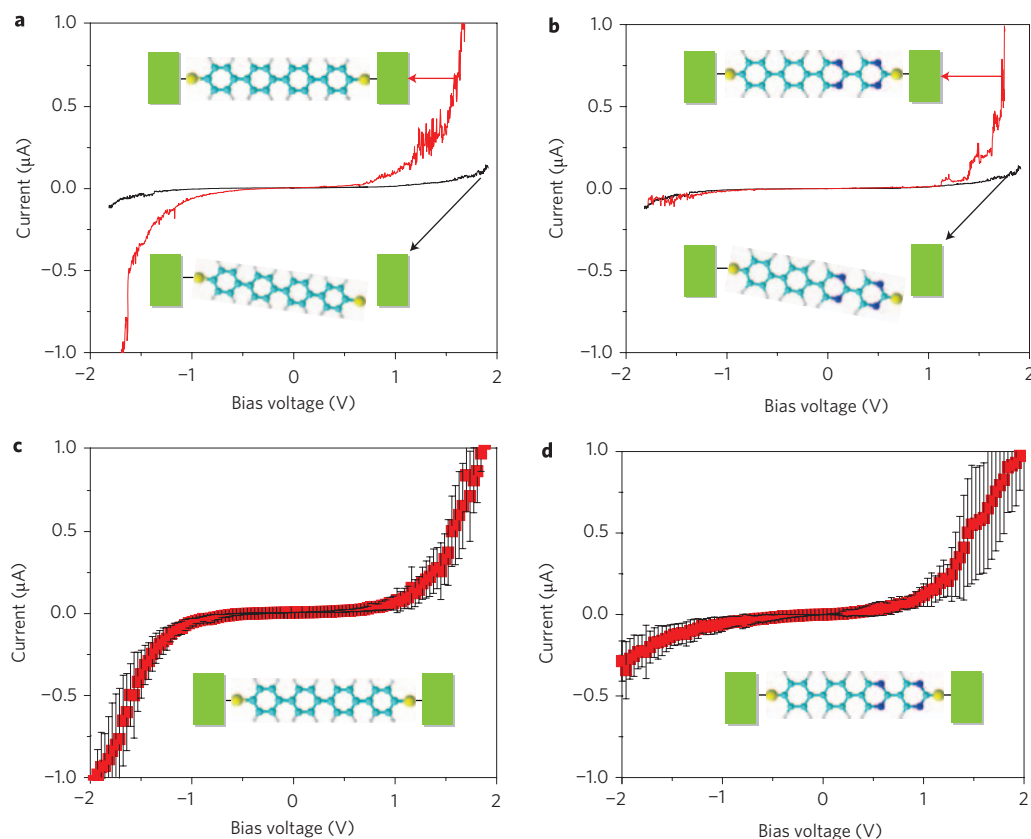
Figure 4 | Current-voltage (*I–V*) curves for the symmetric and non-symmetric molecules. a,b, The *I–V* curves were recorded in both regions A (gap junction, black) and B (single-molecule junction, red) of Fig. 3 for the symmetric tetraphenyl (**a**) and the non-symmetric dipyrimidinyl–diphenyl (**b**) molecules. **c,d**, Average curves for the single-molecule junctions built from 30 (**c**) and 50 (**d**) individual *I–V* curves, with error bars that represent standard deviation.

substrate electrodes. There is a run-to-run variation in the *I–V* curves for the molecular bridge (red curve), as shown in Fig. 4c. Despite the variations, the average *I–V* curve is symmetric. A symmetric molecule does not necessarily result in symmetric *I–V* curves. This is because, although the molecule is symmetric and both the tip and substrate electrodes are gold, different binding sites of the thiol anchor groups at the two gold electrodes may still lead to non-symmetric junctions. Our study shows that this contact-induced non-symmetry does not give rise to significant non-symmetry in the *I–V* characteristic, which is in good agreement with previous work[18].

We have carried out similar measurements on the non-symmetric diphenyl–dipyrimidinyl molecule. In contrast to the symmetric tetraphenyl block, the *I–V* curves for the non-symmetric molecule bridged between the tip and the substrate display strong rectification (Figs 4b,d). The forward current sharply increases to a few microamps at high bias voltages, and the average rectification ratio at a 1.5 V bias is about five to one from positive to negative bias polarities (Fig. 4d), with the forward current flowing from the tip to the substrate. As the molecules are adsorbed onto the gold substrate with the dipyrimidinyl group pointing upward (Fig. 1b), the forward-current direction is from the dipyrimidinyl to the diphenyl block.

To ensure that the orientation of the molecules does not change during the measurement, we analysed the polarities of the individual *I–V* curves and found that more than 90% of the curves had the same rectification polarity, which indicates that the orientation remains largely unchanged during the assembly process and measurements. The non-symmetric molecule has a built-in electric field (dipole[8]) pointing from diphenyl to dipyrimidinyl and the forward current flows against the dipole when the external bias reduces the built-in field, thus resembling a conventional *p–n*

junction. However, despite very similar functionalities, the mechanism for the rectification of the molecular diode is different from that of the conventional *p–n* junctions, as we discuss later.

We have also investigated the charge-transport measurement when the molecule is attached to only one of the two electrodes (gold–molecule–gap–gold) and found that the a.c. response was high (regime A in Fig. 3). As shown in Fig. 4a,b (black curves), the current is low and the *I–V* curves are symmetric for both the symmetric and non-symmetric molecules. This finding emphasizes the importance of providing good contact at both ends of the molecule to observe the rectification effect (see also Supplementary Fig. S3).

The molecular junction has a finite lifetime, even at a small bias, because of the breakdown of the molecule–electrode contact at room temperature[19]. The breakdown process accelerates when the bias increases (a higher current flows through the molecule). Figure 5a shows such a breakdown event occurring during the *I–V* measurement of a tetraphenyl junction. The breakdown is reflected by a sudden drop in the current, and consequently the *I–V* curve returns to the characteristic *I–V* curve for an open tunnelling junction (see Fig. 4). Previously, we observed evidence of current-induced local heating of single-molecule junctions[19,20]. More recently, several other groups, using different methods, have also found substantial local heating in molecular devices[21,22]. As the increase in local temperature accelerates the bond-breaking process, instability at high biases is expected. However, a different breakdown process was also observed, mostly in the non-symmetric molecule, during the sharp current increase in the forward polarity. Instead of an abrupt decrease in the current, a high bias in the forward current direction often caused a sudden and irreversible increase in the current (Fig. 5b). The current quickly becomes so large that it saturates the current
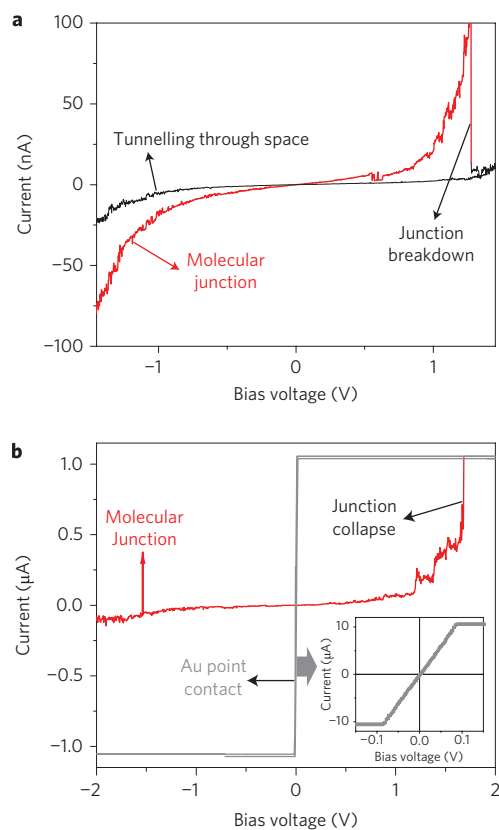
Figure 5 | Two types of instability behaviours of the molecular junctions. **a**, Open-circuit instability, in which the current drops abruptly and the *I–V* curve returns to the open tunnelling gap characteristic. **b**, Short-circuit instability, in which a gold point contact forms during the forward-bias scan; the inset is an expansion of the small bias region to show the linear *I–V* curve for the gold point contact.

Table 1 | Statistical analysis of the occurrence of the collapse of molecular junctions.

Event frequency (%)	Averaged breakdown bias (V)	Current threshold (μA)	Conductance of the gold neck (μS)
70	1.79 ± 0.11	0.72 ± 0.17	80.2 ± 4.68
30	1.75 ± 0.28	0.84 ± 0.12	144.2 ± 12.1

In 15 different *I–V* experiments junction short-circuits were observed in about 40–50% of the total *I–V* characteristics.

ionized at the anode, and the gold ions migrate and deposit on the cathode. In the absence of electrolytes, ionization of gold is very unlikely. However, it has been reported that molten gold can be ionized under an intense electric field[28]. A possible mechanism for the formation of a quantum point contact in our system is that the large current induces substantial local heating of the gold contacts, which, together with the large electric field, results in the ionization and migration of gold between the two electrodes. A microscopic model that can explain the observed instability is yet to be developed, but the observed short-circuit instability at high currents is important for potential device applications.

We carried out theoretical calculations of charge transport[29] using density functional theory within the Perdew, Burke and Ernzerhof generalized gradient approximation[30] to elucidate the rectification mechanism of the dipyrimidinyl–diphenyl diblock. A comprehensive description of the method and findings will be published elsewhere (see Supplementary Information for more details). Briefly, we found that the charge transport occurs through the hole resonant tunnelling mechanism, based on the calculated ionization potential and electron affinity of the molecule, which correspond to the hole and electron energy levels closest to the Fermi level of the electrodes (Fig. 6a).

The calculated *I–V* characteristic for the dipyrimidinyl–diphenyl molecule (Fig. 6b) displays rectification behaviour with the forward current in the dipyrimidinyl–diphenyl direction (positive bias). The characteristic feature of the theoretical *I–V* curve is the non-symmetry in turn-on voltages, that is, the current starts to increase rapidly at $V_{bias} \sim +0.7$ V and ~ -1.2 V. The theoretical rectification ratio at 1.5 V is 2.5, which is smaller than but of the same order of magnitude as the experimental value. The rectification behaviour of the dipyrimidinyl–diphenyl molecule results from the strong non-symmetrical localization of the hole ground state wave function in the applied electric field (Fig. 6a, mechanism i). At zero bias, the hole wave function is strongly localized at the biphenyl end of the molecule near the sample. This is the consequence of the original electronic structure, which reflects the underlying chemical differences between the dipyrimidinyl and diphenyl blocks. Upon application of bias, the wave function non-symmetry results in the non-symmetry of the probability of the hole transfer from the anode to the molecule (γ_{anode}), $\gamma_{anode}^{V>0} > \gamma_{anode}^{V<0}$ (Fig. 6a). The theory explains not only the rectification, but also the polarity of the rectification behaviour.

Conclusions

We have studied charge transport through symmetric tetraphenyl block molecules and non-symmetric dipyrimidinyl–diphenyl diblock molecules covalently bridged between two gold electrodes using an a.c.-assisted STM break-junction method. Despite the similar lengths and structures of the two systems, the conductance of the non-symmetric molecule is three times greater than that of the symmetric one. Whereas the tetraphenyl block displays a perfect symmetric behaviour, the diblock molecule exhibits pronounced rectification behaviour, with a larger current from the dipyrimidinyl to the diphenyl block. Measurements recorded with the non-symmetric molecules bound only to one electrode also

amplifier. After the irreversible current jump, the conductance at small bias is of the order G_0, which corresponds to the formation of a gold point contact between the tip and substrate electrodes. We found that this type of instability occurs in 40–50% of the junctions at a threshold bias voltage of ~1.8 V with a corresponding current slightly below 1 μA (see Table 1). The statistical analysis also shows that the most frequent conductance values after this second type of breakdown are G_0 and $2G_0$. Furthermore, we carried out the measurements in vacuum at low temperature (~10 K, see Supplementary Fig. S5b) and also observed the formation of the gold point contact at large forward-bias voltages.

Current-induced short circuits have been observed in other systems. For example, Stewart *et al.* reported the formation of metal filaments in cross-wire molecular junctions, in which a molecular layer is sandwiched between two metal wires[23]. Teramae *et al.* observed current-induced short circuits in gold–benzenedithiol–gold junctions[24]. The mechanism of the short-circuit instability in these systems is not fully understood. In our measurements, the formation of gold point contacts occurs only in the forward-bias direction in which the current is large, and not at the reverse polarity. This observation indicates that the current is at least partially responsible for the observed instability. Current may lead to instability of a molecular junction by either local heating[19–22] or current-induced force (electromigration)[25,26], but both effects should result in the breakdown of the molecular junctions and create an open circuit, rather than form a metal point contact (short circuit). In electrolytes, a quantum point contact can form by applying a voltage between two gold electrodes separated by a small gap[27]. This interesting phenomenon occurs because gold is
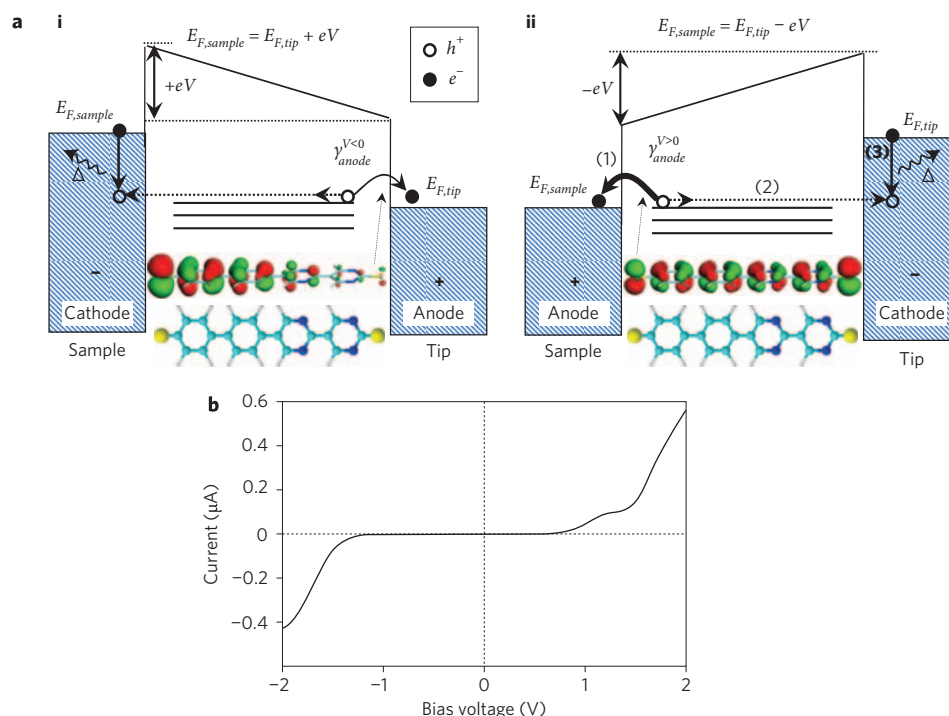
Figure 6 | Representation of the rectification mechanism for the non-symmetric molecule. a, Conduction mechanism for the metal–dipyrimidinyl–diphenyl–metal junction. The right electrode (STM tip) is kept grounded, and the left electrode (substrate) is biased either positively (**ii**) or negatively (**i**). The conduction process is (1) an electron transfers from the electron-rich diphenyl block to the anode, which generates a hole in the molecule, (2) the generated hole transfers under an electric field to the cathode and (3) the injected hole in the cathode recombines with an electron of higher energy (releasing heat at the electrode). The non-symmetry in I–V characteristics is caused by the non-symmetrical behaviour of the hole wave function as a function of the applied electric field. The hole orbitals at $V = -1$ V (**i**) and $V = 1$ V (**ii**) are shown together with the corresponding probabilities of the hole transfer from the anode to the molecule ($\gamma_{anode} \propto |\psi_h(r_a)|^2$), which are such that $\gamma_{anode}^{V>0} > \gamma_{anode}^{V<0}$. E_F, ψ_h and r_a are the Fermi energy of the gold electrodes, the hole wave-function and the anode spatial coordinate, respectively. **b**, Calculated I–V characteristics (see Supplementary Information for more details).

display symmetric I–V curves, which emphasizes the importance of the molecule–electrode contact in the rectification effect. We have performed first-principle calculations of charge transport through the dipyrimidinyl–diphenyl molecule and provided an explanation for the mechanisms of the observed rectification and polarity. At large forward currents (a few microamps), the gold–molecule–gold junction for the non-symmetric molecule becomes unstable through the formation of gold point contacts between the two electrodes.

Methods

The two different molecules studied, symmetric tetraphenyl (Fig. 1a) and non-symmetric dipyrimidinyl–diphenyl blocks (Fig. 1b), were synthesized according to a reported procedure[8]. The molecules are terminated with thiols so that they can bind to two electrodes and form a gold–molecule–gold junction. SAMs on a gold substrate were prepared for both systems using different procedures. In the first case, deprotection of the two symmetric trimethylsilylethyl groups was carried out in a single step using tetrabutylammonium fluoride as the cleaving reagent in an argon-purged tetrahydrofuran (THF) solution that contained 50 μM of the target molecule (Fig. 1a). At the same time, a gold substrate prepared using the procedure described below was immersed in the solution for more than 10 hours. Then, the substrate was rinsed successively with THF, hexane and ethanol and dried with nitrogen after each rinsing step.

The SAM of the non-symmetric molecule was prepared in two steps (see Fig. 1b). The first step deprotected the cyanoethyl group using sodium ethoxide as the cleaving reagent in an argon-purged ethanol–THF mixture. A gold substrate was immediately immersed for 10 hours in the solution that contained the molecules. After the formation of the SAM, the gold substrate was rinsed thoroughly with THF and then with ethanol. At this stage, STM break-junction measurements were carried out as control experiments to verify that no molecular bridges could be formed in the presence of the top trimethylsilylethyl protecting group (see Supplementary Fig. S4). To carry out the second deprotection step, the sample was transferred into an argon-purged THF solution to remove the protecting group using the same procedure as that for the symmetric molecule. This second deprotection reaction lasted over seven hours, after which the gold substrate was rinsed with hexane and ethanol several times and the residual solvent removed by blowing with nitrogen.

The gold substrates were prepared by thermally evaporating 130 nm of gold (99.999%, Alfa Aesar) on freshly cleaved mica slides (Ted Pella) in an ultra-high vacuum chamber (5×10^{-8} torr). Before each measurement, the gold electrode was annealed briefly in a hydrogen flame to remove any possible contamination and to generate large, atomically flat terraces. SAMs were characterized with an STM that showed large, uniform and flat terraces separated by 0.23 nm high atomic steps of the gold(111) (Fig. 1c). A closer view (Fig. 1c, inset) shows pinholes on the flat terraces, which are characteristic features of the formation of a thiol–gold bond.

The experiments were performed with a previously described STM break-junction setup[6]. Briefly, freshly etched gold tips were prepared from a 0.25 mm gold wire (99.998% Alfa Aesar) in a hydrochloric acid/ethanol (1/1) bath. The experiments were carried out in non-polar solvents, mesitylene (>99.0%, Fluka) and toluene (>99.5%, Mallinckrodt Chemicals), which reduced possible surface contamination. Before use, the STM Teflon cell was soaked in boiling piranha for 20 minutes, then thoroughly rinsed with pure water (resistivity of 18 MΩ cm). After drying with N₂, the cell was placed over the gold–SAM surface and filled with 80 μl of solvent. A typical break-junction experiment comprised a total of 2,000–2,500 current–distance traces collected at pulling rates of 20–40 nm s⁻¹. Of these traces, 8–10% displayed plateaus that corresponded to the formation of a molecular bridge and were employed to build the histograms. The break-junction experiments were performed at different biases (within the ±150 mV range) to check the consistency of the measured molecular conductance values (G).

The a.c.-modulation assisted method was performed by applying a sinusoidal function to the Z piezo to create a 0.02–0.08 nm modulation of the tip–substrate distance at 2 kHz frequency. Typically, we started the experiment with a low setpoint current to ensure the tip-substrate distance was larger than the molecular length. (The tip–sample distance was roughly estimated from a classical one-dimensional tunnelling gap for the STM junction with a local energy barrier $\phi_B = 1$ eV for Au (ref. 31). The molecular lengths considered for C8-dithiol and conjugated blocks are 0.8 and 1.9 nm, respectively.) Thus, no molecules could bridge between the tip and substrate electrodes, and tunnelling through the space between the tip and the SAM-covered substrate dominated the current, which was evidenced by a large a.c. response caused by the sharp dependence of the tunnelling current with distance. The setpoint was then gradually increased to reduce the tip–substrate distance below the molecular length so that molecules could bridge between both electrodes. During this process, a very small feedback gain was applied, which could correct slow drift but not the a.c. response. The formation of a molecular bridge led to a sudden and

large reduction in the a.c. response. d.c. jumps and *I–V* characteristics during the molecular bridge formation were then determined by turning off the feedback gain. *I–V* curves were collected from the d.c. versus applied bias voltage, and the simultaneously recorded a.c. response ensured that the molecular bridge was intact during the measurement.

References

1. Aviram, A. & Ratner, M. A. Molecular rectifiers. *Chem. Phys. Lett.* **29**, 277–283 (1974).
2. Martin, A. S., Sambles, J. R. & Ashwell, G. J. Molecular rectifier. *Phys. Rev. Lett.* **70**, 218–221 (1993).
3. Chabinyc Michael, L. *et al*. Molecular rectification in a metal–insulator–metal junction based on self-assembled monolayers. *J. Am. Chem. Soc.* **124**, 11730–11736 (2002).
4. Elbing, M. *et al*. A single-molecule diode. *Proc. Natl Acad. Sci. USA* **102**, 8815–8820 (2005).
5. Smit, R. H. M. *et al*. Measurement of the conductance of a hydrogen molecule. *Nature* **419**, 906–909 (2002).
6. Xu, B. & Tao, N. J. Measurement of single-molecule resistance by repeated formation of molecular junctions. *Science* **301**, 1221–1223 (2003).
7. Lee, Y., Carsten, B. & Yu, L. Understanding the anchoring group effect of molecular diodes on rectification. *Langmuir* **25**, 1495–1499 (2009).
8. Morales, G. M. *et al*. Inversion of the rectifying effect in diblock molecular diodes by protonation. *J. Am. Chem. Soc.* **127**, 10456–10457 (2005).
9. Venkataraman, L., Klare, J. E., Nuckolls, C., Hybertsen, M. S. & Steigerwald, M. L. Dependence of single-molecule junction conductance on molecular conformation. *Nature* **442**, 904–907 (2006).
10. Li, X. *et al*. Conductance of single alkanedithiols. Conduction mechanism and effect of molecule–electrode contacts. *J. Am. Chem. Soc.* **128**, 2135–2141 (2006).
11. He, J., Fu, Q., Lindsay, S., Ciszek, J. W. & Tour, J. M. Electrochemical origin of voltage-controlled molecular conductance switching. *J. Am. Chem. Soc.* **128**, 14828–14835 (2006).
12. Xiao, X., Xu, B. & Tao, N. J. Measurement of single molecule conductance: benzenedithiol and benzenedimethanethiol. *Nano Lett.* **4**, 267–271 (2004).
13. Xu, B., Xiao, X. & Tao, N. J. Measurements of single-molecule electromechanical properties. *J. Am. Chem. Soc.* **125**, 16164–16165 (2003).
14. Xu, B. Modulating the conductance of a Au–octanedithiol–Au molecular junction. *Small* **3**, 2061–2065 (2007).
15. Xia, J. L., Díez-Perez, I. & Tao, N. J. Electron transport in single molecules measured by a distance–modulation assisted break junction method. *Nano Lett.* **8**, 1960–1964 (2008).
16. Haiss, W. *et al*. Precision control of single-molecule electrical junctions. *Nat. Mater.* **5**, 995–1002 (2006).
17. Haiss, W. *et al*. Measurement of single molecule conductivity using the spontaneous formation of molecular wires. *Phys. Chem. Chem. Phys.* **6**, 4330–4337 (2004).
18. Reichert, J. *et al*. Driving current through single organic molecules. *Phys. Rev. Lett.* **88**, 176804/1–176804/4 (2002).
19. Huang, Z. *et al*. Local ionic and electron heating in single-molecule junctions. *Nature Nanotech.* **2**, 698–703 (2007).
20. Huang, Z., Xu, B., Chen, Y., Di Ventra, M. & Tao, N. Measurement of current-induced local heating in a single molecule junction. *Nano Lett.* **6**, 1240–1244 (2006).
21. Tsutsui, M., Taniguchi, M. & Kawai, T. Local heating in metal–molecule–metal junctions. *Nano Lett.* **8**, 3293–3297 (2008).
22. Ioffe, Z. *et al*. Detection of heating in current-carrying molecular junctions by Raman scattering. *Nature Nanotech.* **3**, 727–732 (2008).
23. Stewart, D. R. *et al*. Molecule-independent electrical switching in Pt/organic monolayer/Ti devices. *Nano Lett.* **4**, 133–136 (2004).
24. Teramae, Y. *et al*. High-bias breakdown of Au/1,4-benzenedithiol/Au junctions. *Appl. Phys. Lett.* **93**, 083121 (2008).
25. Strachan, D. R. *et al*. Controlled fabrication of nanogaps in ambient environment for molecular electronics. *Appl. Phys. Lett.* **86**, 043109 (2005).
26. Esen, G. & Fuhrer, M. S. Temperature control of electromigration to form gold nanogap junctions. *Appl. Phys. Lett.* **87**, 263101 (2005).
27. Boussaad, S. & Tao, N. J. Atom-size contacts and gaps between electrodes fabricated with a self-terminated electrochemical method. *Appl. Phys. Lett.* **80**, 2398–2400 (2002).
28. Thompson, S. P. & von Engel, A. Field emission of metal ions and microparticles. *J. Phys. D.* **15**, 925–931 (1982).
29. Oleynik, I. I., Kozhushner, M. A., Posvyanskii, V. S. & Yu, L. Rectification mechanism in diblock oligomer molecular diodes. *Phys. Rev. Lett.* **96**, 096803 (2006).
30. Perdew, J. P., Burke, K. & Ernzerhof, M. Generalized gradient approximation made simple. *Phys. Rev. Lett.* **77**, 3865–3868 (1996); *erratum* **78**, 1396 (1997).
31. Nagy, G., Mayer, D. & Wandlowski, T. Distance tunnelling characteristics of solid/liquid interfaces: Au(111)/Cu$_2$ + /$_{H2SO4}$. *PhysChemComm* **5**, 112–116 (2002).

Acknowledgements

Author contributions

N.J.T. and L.Y. conceived this project. I.D.-P. and J.H. conducted experiments and analysed data. Y.L. synthesized the molecules. I.I.O. designed and supervised the theoretical study and L.A. and M.A.K. did the calculations.

Additional information

Supplementary information accompanies this paper at www.nature.com/naturechemistry. Reprints and permission information is available online at http://npg.nature.com/reprintsandpermissions/. Correspondence and requests for materials should be addressed to L.Y. and N.T.